crystals

MDPI

Article

Simultaneous Improvement in Dissolution Behavior and Oral Bioavailability of Naproxen via Salt Formation

Xian-Rui Zhang [1,*], Bao-Lin Wu [2], Jing-Jing Han [1] and Jin-Qing Li [1]

[1] College of Food and Pharmaceutical Engineering, Wuzhou University, Wuzhou 543000, China; 18240862704@163.com (J.-J.H.); 18775024042@163.com (J.-Q.L.)
[2] Guangxi Wuzhou Zhongguan Inspection Technology Services Co., Limited, Wuzhou 543000, China; 18269213580@163.com
* Correspondence: zhangyang159246@163.com

Abstract: Naproxen (NAP) is a non-steroidal anti-inflammatory drug (NSAID) that belongs to the arylpropionic acid class. Classified as a Biopharmaceutical Classification System (BCS) class II drug, NAP exhibits low water solubility, thus resulting in restricted oral bioavailability. This study aimed to evaluate the effectiveness of pharmaceutical salts in enhancing the solubility and oral bioavailability of NAP. Two novel NAP salts, specifically naproxen-ethylenediamine (NAP-EDA) and naproxen-trometamol (NAP-TRIS), were synthesized using a 2:1 and 1:1 stoichiometric ratio, respectively. The NAP-EDA and NAP-TRIS powders were thoroughly characterized using single-crystal X-ray diffraction (SXRD), powder X-ray diffraction (PXRD) and differential scanning calorimetry (DSC), providing a comprehensive understanding of their structural and thermal properties. Additionally, the solubilities and dissolution rates of NAP-EDA and NAP-TRIS salts were assessed in water and a pH 6.86 phosphate buffer. Notably, the solubility of NAP-TRIS salt increased markedly, by 397.5-fold in water and 6.2-fold at pH 6.86. Furthermore, in vivo pharmacokinetic studies in rats revealed that NAP-TRIS salt displayed faster absorption and higher peak blood concentrations compared to NAP. These results indicate that the NAP-TRIS salt effectively enhanced the solubility and oral bioavailability of naproxen. In conclusion, this study underscores the potential of pharmaceutical salts, particularly NAP-TRIS, in improving the solubility and oral bioavailability of drugs with low aqueous solubility, presenting a promising avenue for advancing drug delivery and therapeutic outcomes.

Keywords: naproxen; ethylenediamine; trometamol; salt; solubility; bioavailability

check for updates

Citation: Zhang, X.-R.; Wu, B.-L.; Han, J.-J.; Li, J.-Q. Simultaneous Improvement in Dissolution Behavior and Oral Bioavailability of Naproxen via Salt Formation. *Crystals* **2024**, *14*, 1104. https://doi.org/10.3390/cryst14121104

Academic Editor: Changquan Calvin Sun

Received: 6 November 2024
Revised: 18 December 2024
Accepted: 20 December 2024
Published: 23 December 2024

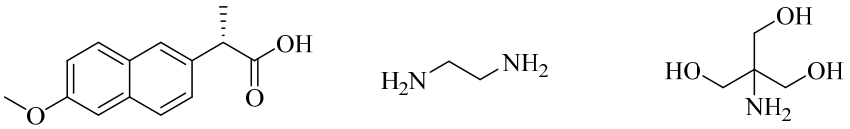
Copyright: © 2024 by the authors. Licensee MDPI, Basel, Switzerland. This article is an open access article distributed under the terms and conditions of the Creative Commons Attribution (CC BY) license (https://creativecommons.org/licenses/by/4.0/).

1. Introduction

Drug cocrystals and salts play a significant role in drug discovery and development, as well as in the preparation of dosage forms, ultimately leading to improved therapeutic efficacy [1–5]. By increasing drug bioavailability, reducing both the dose and frequency of administration and enhancing patient compliance, drug cocrystals and salts offer numerous advantages [6–10]. Notably, drug salts have the ability to modify the physicochemical properties of drugs, thereby enhancing their solubility, stability, and overall therapeutic efficacy [11–20].

Naproxen is an arylpropionic non-steroidal anti-inflammatory drug that possesses anti-inflammatory, analgesic, and antipyretic effects, and is primarily used to treat pain caused by rheumatic and rheumatoid arthritis, osteoarthritis, and gout [21–23]. The chemical structure of NAP is shown in Figure 1, and its IUPAC name is α-methyl-6-methoxy-2-naphthaleneacetic acid. However, its low solubility results in poor bioavailability, which affects its absorption in the body and reduces its effectiveness [24,25]. Numerous NAP cocrystals and salts with nicotinamide [26,27], isonicotinamide [28], picolinamide [29,30], duloxetine [31], L-alanine [32], D-alamine, D-tyrosine, and D-tryptophan [33], arginine [34], zwitterionic prolinium [35], tramadol [36], bipyridine and piperazine [37], 4-amino pyridine and

2-amino pyridine [38], urea and thiourea [39], (1R,2R)-1,2-diphenylethylenediamine [40], caprolactam and oxymatrine [41] and vortioxetine [42] have been reported to improve its solubility and bioavailability. However, the potential for these coformers to be marketed as pharmaceutical formulations is limited due to their toxicity, non-pharmaceutical excipients, or absence of a single-crystal structure. In this study, we have chosen trometamol and ethylendediamine (Figure 1) as a viable coformer with proven medicinal applications in drug solid-state chemistry, biopharmaceutical properties, and drug formulation [43–48]. Notably, there have been successful cases of non-steroidal anti-inflammatory drugs marketed with trometamol salts, such as ketoglutarate trometamol salt and dextroketoprofen trometamol salt.



Naproxen (NAP) Ethylenediamine (EDA) Trometamol (TRIS)

Figure 1. Molecule structures of NAP, EDA, and TRIS.

The present study aimed to develop novel and safe salt forms with improved solubility and bioavailability. The synthesis of NAP-EDA and NAP-TRIS salts was performed, followed by thorough characterization using various techniques such as single-crystal X-ray diffraction (SXRD), powder X-ray diffraction (PXRD), and differential scanning calorimetry (DSC). Additionally, we evaluated the solubility and bioavailability of the salts for pharmaceutical applications.

2. Results

2.1. Crystal Structure Analysis

We have successfully synthesized two suitable single-crystal X-ray diffraction (SXRD) salts of naproxen, namely NAP-EDA salt (2:1) and NAP-TRIS salt (1:1), using the slow evaporation method. Tables 1 and 2 have summarized the detailed crystallographic and hydrogen bond data for the two synthesized salts. The corresponding CIF files have been deposited in the Cambridge Structural Database.

Table 1. Crystallographic parameters of NAP-EDA and NAP-TRIS salts.

	NAP-EDA	**NAP-TRIS**
Empirical formula	$2(C_{14}H_{13}O_3)\bullet C_2H_{10}N_2$	$C_{14}H_{13}O_3\bullet C_4H_{12}NO_3$
Molecule weight	520.61	351.39
Temperature (K)	293(2)	293(2)
Crystal system	Monoclinic	Orthorhombic
space group	*I*2	$P2_12_12_1$
a (Å)	12.5633(12)	6.3167(10)
b (Å)	6.0077(8)	8.5152(17)
c (Å)	36.747(4)	33.133(5)
α (°)	90	90
β (°)	99.720(9)	90
γ (°)	90	90
Volume ($Å^3$)	2733.7(5)	1782.2(5)
Z	4	4
Density (g/cm^3)	1.265	1.310
R_1/wR_2 [$I > 2\sigma(I)$]	0.0709/0.1273	0.0618/0.0918
GOF	0.940	0.991
Larg peak and hole ($e/Å^3$)	0.164/−0.190	0.183/−0.200
CCDC	2,391,216	2,306,212

Table 2. Hydrogen bonding distances (Å) and angles (°) for the NAP-EDA and NAP-TRIS salts.

Compound	D-H···A	d(D-H)	d(H···A)	d(D···A)	<(DHA)	Symmetry Code
NAP-EDA	$N1^+$-H1A···O1	0.88	1.93	2.732(10)	152	−x − 1, y + 1, −z
	$N1^+$-H1B···O5	0.88	1.91	2.791(10)	176	x, y + 1, z
	$N1^+$-H1C···O4	0.87	1.89	2.757(10)	173	−x − 2, y + 1, −z
	$N2^+$-H2A···O5	0.87	2.00	2.786(10)	150	x, y, z
	$N2^+$-H2B···O1	0.87	1.83	2.702(10)	177	−x − 1, y, −z
	$N2^+$-H2C···O2	0.87	1.90	2.753(10)	164	x, y, z
NAP-TRIS	$N1^+$-H1B···O4	0.89	2.07	2.950(4)	169	x − 1/2, −y − 3/2, −z
	$N1^+$-H1A···O1	0.89	1.86	2.746(4)	170	x + 1/2, −y − 3/2, −z
	$N1^+$-H1C···O6	0.89	2.01	2.896(4)	174	x − 1/2, −y − 1/2, −z
	O4-H4···O1	0.82	1.83	2.644(3)	168	x, y, z
	O5-H5A···O2	0.82	1.81	2.621(3)	172	x, y + 1, z
	O6-H6···O5	0.82	1.89	2.685(3)	162	x + 1, y, z

2.1.1. NAP-EDA Salt (2:1)

NAP-EDA salt crystallized in the monoclinic crystal system with the *I*2 space group. In the crystal structure, the asymmetric unit consisted of two independent NAP anions and one bivalent EDA cation. Notably, both independent NAP molecules exhibited the S configuration (Figures S1 and S2). The NAP anions and EDA cations arranged themselves in a sandwich-like structure facilitated by the intramolecular hydrogen bonds $N1^+$-H1A···O1, $N1^+$-H1B···O5, $N1^+$-H1C···O4, $N2^+$-H2A···O5, $N2^+$-H2B···O1 and $N2^+$-H2C···O2 (Figure 2).

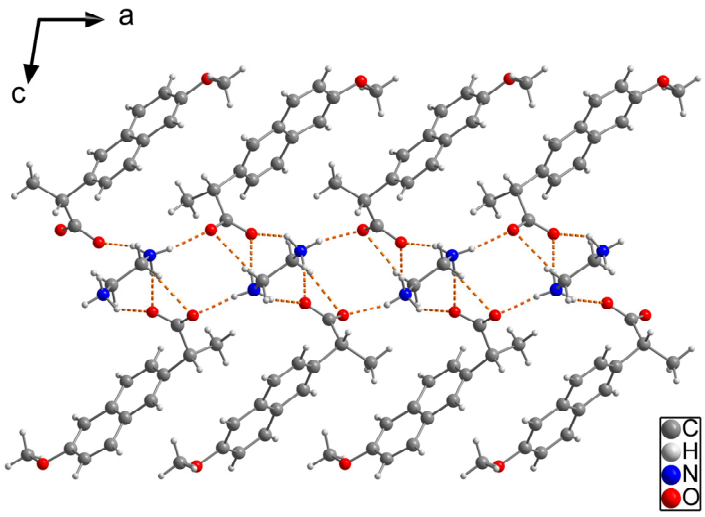


Figure 2. The 3D sandwich-like structure of NAP-EDA salts.

2.1.2. NAP-TRIS Salt (1:1)

NAP-TRIS salt crystallized in the orthorhombic crystal system with the $P2_12_12_1$ space group. In the crystal structure, the asymmetric unit consisted of one S-configured NAP anion and one TRIS cation. The TRIS cations formed a two-dimensional laminar arrangement through $N1^+$-H1B···O4, $N1^+$-H1C···O6 and O6-H6···O5 intramolecular hydrogen bonds (Figure 3a). Furthermore, the laminar structures and the NAP anions were interconnected via $N1^+$-H1A···O1, O4-H4···O1 and O5-H5A···O2 intermolecular hydrogen bonds. These interactions resulted in the formation of three-dimensional sandwich-type assemblies along the *b*-axis direction (Figure 3b, Figures S3 and S4).

It is worth noting that due to the presence of only light atoms in the structure, X-ray analysis alone cannot determine the absolute configuration. Therefore, when purchasing the naproxen sample, we deliberately chose the S-configuration naproxen to ensure consistency and accuracy in our experiments.

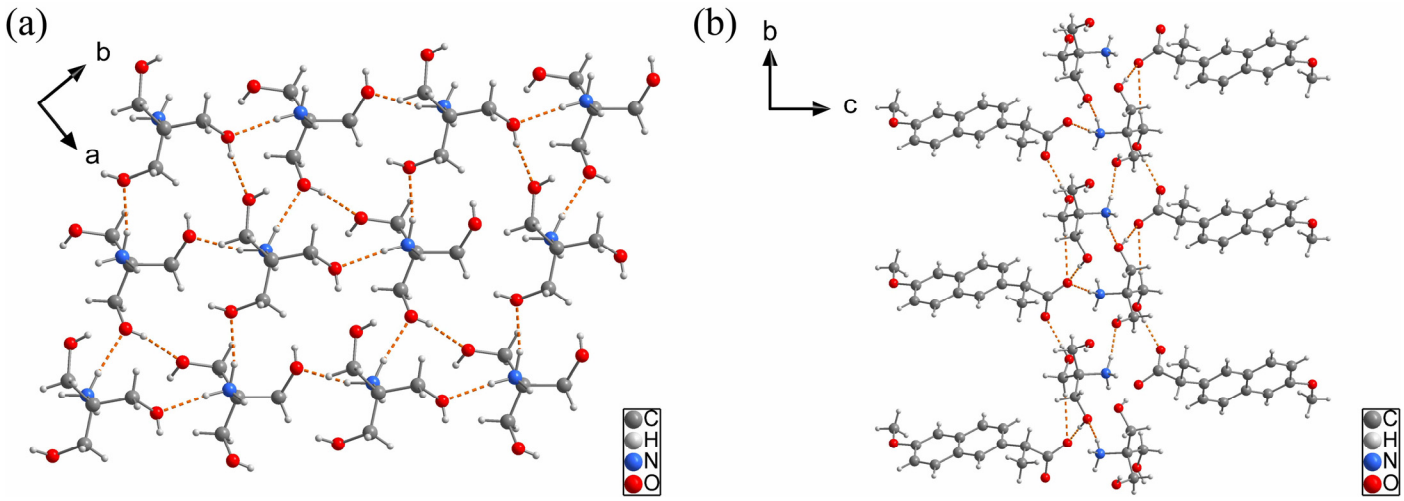


Figure 3. (**a**) The 2D laminar structure produced by the TRIS cations; (**b**) the 3D sandwich-type arrangement of NAP-TRIS salts, viewing from the *b* axis.

It is well known that NAP is a non-steroidal anti-inflammatory drug with low water solubility. The low water solubility of NAP (CCDC reference: 1,130,671) can be attributed to two factors. Firstly, the structure of NAP contains mainly hydrophobic functional groups. Secondly, NAP possesses a hydrophilic group (carboxylic acid group) that is connected through intermolecular hydrogen bonding and trapped within the hydrophobic groups (Figure 4). When the NAP-EDA and NAP-TRIS salt are formed, the original hydrogen bond structure is disrupted, allowing the hydrophobic groups of NAP to be released. This structural change elucidates the enhancement of NAP's water solubility in the presence of NAP-EDA and NAP-TRIS salts.

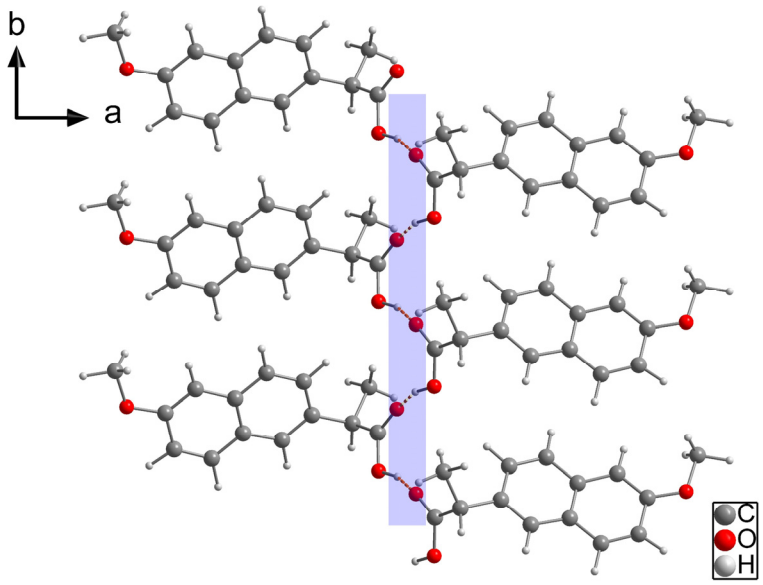


Figure 4. The carboxyl portion of NAP was trapped under hydrophobic group.

2.2. Powder X-Ray Diffraction (PXRD) Analysis

The experimental PXRD pattern of the NAP-EDA and NAP-TRIS salts distinctly differed from that of NAP (Figure 5). Specifically, the NAP-EDA salt displayed a new characteristic peak at 5.06°, 9.92°, 14.82°, 15.98°, 16.84°, 17.56°, 19.84°, 21.14°, 22.38°, 26.70°, and 28.56°. Additionally, the NAP-TRIS salt displayed a novel characteristic peak at 5.18°, 10.52°, 11.54°, 14.16°, 16.02°, 17.38° and 25.20°. Importantly, the experimental PXRD pattern

of both salts closely correlated with the simulated single-crystal structure, reinforcing the successful synthesis of pure NAP salts.

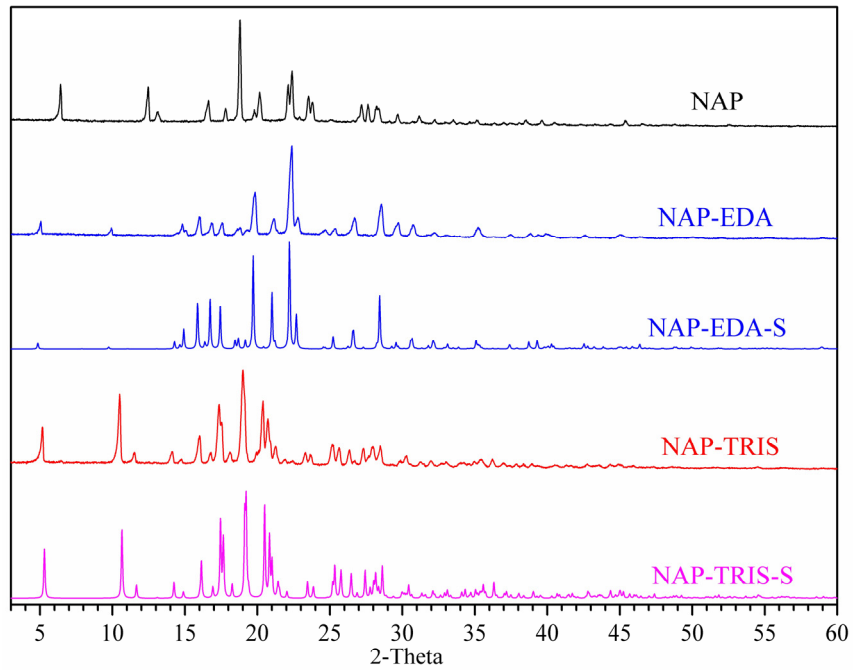


Figure 5. PXRD patterns of NAP, NAP-EDA and NAP-TRIS salts.

2.3. Differential Scanning Calorimetry (DSC) Analysis

The NAP-EDA and NAP-TRIS salts displayed distinct thermodynamic properties when compared to NAP, as shown in Figure 6. Specifically, NAP exhibited heat absorption peaks at 161 °C, attributable to the melting of its raw material. In contrast, the NAP-EDA and NAP-TRIS salts manifested heat absorption peaks at 192 °C and 180 °C, respectively, signifying their individual melting temperatures. Notably, both NAP-EDA and NAP-TRIS salts exhibited superior thermodynamic stability compared to NAP.

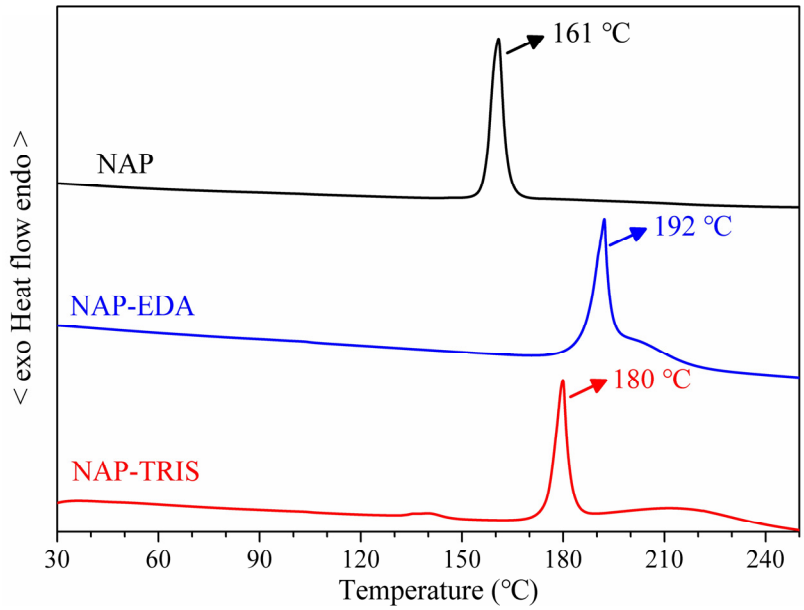


Figure 6. DSC curves of NAP, NAP-EDA and NAP-TRIS salts.

2.4. Solubility and Dissolution Rate Studies

In this study, we investigated the solubility of NAP, NAP-EDA and NAP-TRIS in water (pH = 8.08) and bio-relevant media (pH = 6.86) at 37 °C, and the results were presented in Table 3. The data indicated that the solubility of NAP, NAP-EDA and NAP-TRIS in water was 49.6 mg/L, 3732.5 mg/L, and 19,720.2 mg/L, respectively. In phosphate buffer at pH 6.86, the solubilities of NAP, NAP-EDA and NAP-TRIS were 2771.2 mg/L, 5921.8 mg/L, and 17,218.1 mg/L, respectively. Compared to NAP, both NAP-EDA and NAP-TRIS exhibited significantly enhanced solubility in two media: a 75.2-fold and 397.5-fold increase in water, a 2.1-fold and 6.2-fold increase in the phosphate buffer at pH 6.86. The improved solubility of these drugs facilitates the development of stable liquid dosage forms and high-concentration solid dosage forms, such as orally disintegrating tablets and quick-dissolving tablets, thereby enhancing patient convenience and treatment outcomes.

Table 3. Measured solubility and IDR values of NAP, NAP-EDA and NAP-TRIS salts in water and phosphate buffer (pH 6.86) solutions at 37 °C.

Medium	Compound	Concentration of NAP (mg/L)	IDR (mg/(cm^2·min))	Final pH in Solubility Experiments
water	NAP	49.6 ± 2.2	0.0096	6.88
	NAP-EDA	3732.5 ± 57.0 (×75.2)	0.2093 (×21.8)	6.88
	NAP-TRIS	19,720.2 ± 399.2 (×397.5)	1.6710 (×174.0)	6.72
pH 6.86	NAP	2771.2 ± 37.8	0.3074	6.78
	NAP-EDA	5921.8 ± 157.30 (×2.1)	0.7339 (×2.3)	6.82
	NAP-TRIS	17,218.1 ± 357.2 (×6.2)	3.4899 (×11.3)	6.82

Based on Table 3 and Figure 7, NAP-EDA and NAP-TRIS exhibited higher dissolution rates in water and biologically relevant media compared to NAP. Specifically, in water, NAP-EDA had a dissolution rate 21.8 times higher than NAP, while NAP-TRIS achieved an even higher rate of 174.0 times. This significant improvement is likely attributed to the inclusion of EDA and TRIS ligands, which enhance the hydrophilicity of NAP's surface, thereby increasing its solubility in water. In a phosphate buffer at pH 6.86, though the enhancement in dissolution rate was less pronounced compared to water, NAP-EDA and NAP-TRIS still showed dissolution rates 2.3 and 11.3 times higher than NAP. This indicates that under conditions mimicking the human body's physiological pH, the modified drugs maintained a relatively high dissolution rate, facilitating drug absorption.

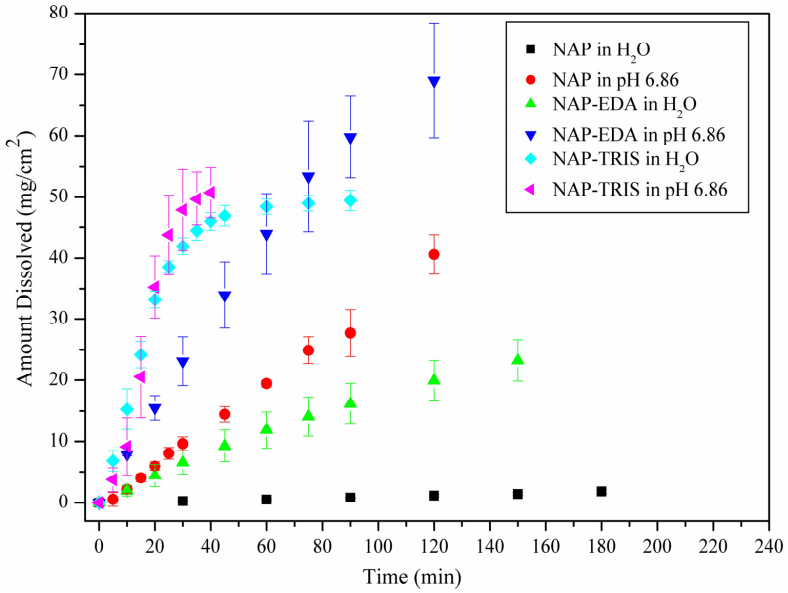


Figure 7. Dissolution profiles for NAP, NAP-EDA and NAP-TRIS salts in water and pH 6.86 solutions.

The stability of the residual samples from the solubility experiments was assessed using PXRD tests (Figures S5–S7). The results demonstrated that the PXRD spectra of NAP and NAP-EDA in both water and bio-relevant media remained unchanged (Figures S3 and S4), indicating their stability in these environments. Moreover, the PXRD spectra of NAP-TRIS salt in water exhibited no alterations (Figure S7), suggesting its stability in this medium as well. However, under the pH 6.86 condition, which mimicked the environment of human intestinal absorption, most of NAP-TRIS salt converted into an amorphous form. This amorphous form could increase the solubility of the drug, making it easier for the human body to absorb and utilize.

In summary, the addition of highly water-soluble ligands EDA and TRIS can significantly improve the solubility and dissolution performance of NAP. This enhancement was observed in water and biologically relevant media, offering valuable insights for drug formulation and clinical use.

2.5. Pharmacokinetic Study

In this study, we assessed the oral absorption of NAP and NAP-TRIS salt in Sprague-Dawley rats, taking into consideration safety and solubility factors. The evaluation of oral bioavailability was performed by analyzing the peak plasma concentration (C_{max}) and area under the curve (AUC) values. The results, presented in Table 4 and Figure 8, showed that NAP-TRIS salt exhibited a higher peak plasma concentration (18.3 µg/mL) in comparison to NAP (17.2 µg/mL). Additionally, the AUC value of NAP-TRIS salt was approximately 1.2 times greater than that of the free NAP form.

Table 4. In vivo pharmacokinetic parameters of NAP and NAP-TRIS salt.

Drug	$T_{1/2}$ (h)	T_{max} (h)	C_{max} (µg/mL)	$AUC_{0\rightarrow24}$ (h*µg/mL)	$MRT_{0\rightarrow t}$ (h)	F (%)
NAP	24.9	4.0	17.2	269.9	16.2	100
NAP-TRIS	28.8	4.0	18.3	319.9	16.6	119

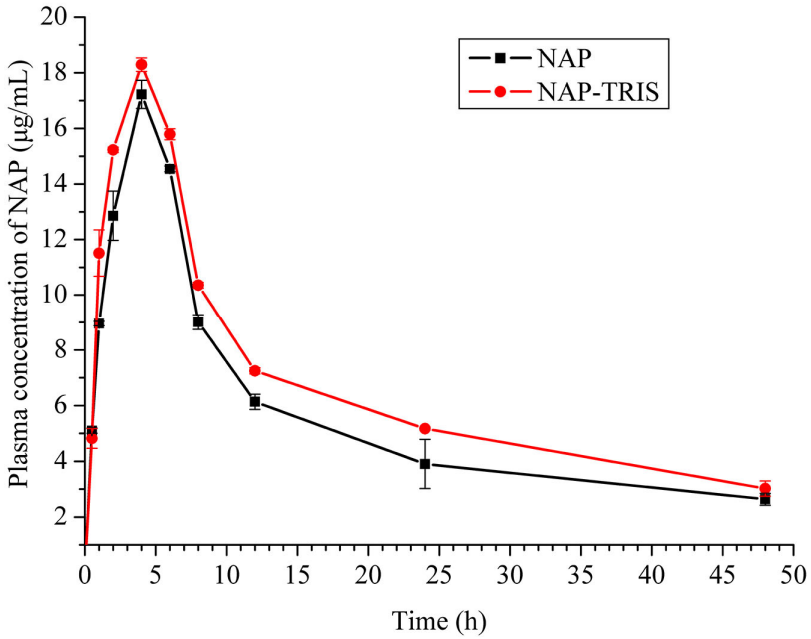


Figure 8. Pharmacokinetic profiles of NAP (black square) and NAP-TRIS (red circle) in male Sprague-Dawley rats. There were n = 6 rats in each group.

Furthermore, the mean retention time ($MRT_{0\rightarrow t}$) for the NAP-TRIS formulation was found to be longer (16.6 h) compared to the free NAP form (16.2 h). These results indicate that the oral bioavailability of naproxen can be enhanced through the use of trometamol

in salt form, which improves solubility and modifies the polar carboxylic group of NAP. Overall, the pharmacokinetic results support the notion that NAP-TRIS salt offers improved oral bioavailability compared to NAP, owing to its enhanced solubility and modified molecular structure.

3. Materials and Methods

3.1. Instrumentations and Materials

NAP (purity > 98%), EDA (purity > 98%) and TRIS (purity > 98%) were purchased from Shanghai Aladdin Biochemical Technology Co., Ltd. (Shanghai, China). The water used in the experiment is Wahaha purified water, with a pH of 8.08, sodium content of 46.3 mg/L, and calcium content of 35.11 mg/L. All reagents (purity > 98%) were purchased from Sinopharm Chemical Reagent Co., Ltd. (Beijing, China). All chemicals and reagents were obtained from various commercial sources and used without further purification. powder X-ray diffraction (PXRD) measurements of NAP, NAP-EDA and NAP-TRIS salts were conducted using a Bruker corporation D8 ADVANCE with a Cu-Kα radiation tube (λ = 1.5418 Å) at 40 mA and 40 kV. The angular range for data collection was 3–60°. Differential scanning calorimetry (DSC) thermograms of NAP, NAP-EDA and NAP-TRIS salts were recorded using a Mettler-Toledo analyzer (Greifensee, Switzerland, Mettler-Toledo Group) in a nitrogen environment from 30 °C to 250 °C at a constant heating rate of 10 °C/min, and the temperature calibration of the DSC is performed using indium. The single-crystal X-ray diffraction (SCXRD) data for the NAP-EDA and NAP-TRIS salts were collected using a Bruker Apex II CCD equipped with Mo-Kα radiation (λ = 0.71073 Å) at a temperature of 293 K. The crystal structures were solved through direct methods and refined with the SHELXL program [49]. All crystal structures are mapped using Diamond version 4.0.0 [50]. The resulting crystal structure parameters, along with hydrogen bond distances and angles, are summarized in Tables 1 and 2.

3.2. Preparation of NAP-EDA and NAP-TRIS Salts

3.2.1. Preparation of NAP-EDA and NAP-TRIS Powder Samples

To prepare the NAP-EDA powder samples, 500 mg of NAP was fully dissolved in 20 mL of acetonitrile, with the subsequent addition of 176 µL of EDA. Stirring the mixture for 30 min resulted in the formation of a considerable quantity of white precipitate. Following filtration, the product was dried to obtain the final NAP-EDA salt sample. The yield was 80.06%.

To prepare the NAP-TRIS powder samples, 200 mg of NAP and 105 mg of TRIS (in a molar ratio of 1:1) were thoroughly mixed in an agate mortar. Afterwards, methanol solvent was added as a co-solvent, and the mixture was ground for 30 min. The resulting mixture was then dried in an oven at 40 °C for 24 h. The dried samples are referred to as the NAP-TRIS samples.

3.2.2. Preparation of NAP-EDA and NAP-TRIS Crystals

A total of 50 mg of the NAP-EDA powder sample was accurately weighed and dissolved in 6 mL of an acetonitrile–water mixture (with a volume ratio of 5:1). Following evaporation of the solution at room temperature for 5 to 7 days, colorless, needle-shaped NAP-EDA crystals were observed.

To prepare the NAP-TRIS crystals, 20 mg of the grinding sample was dissolved in 5 mL of methanol. The mixture was stirred for 30 min and then transferred to a tube to undergo slow evaporation. After 7–10 days, colorless flaky NAP-TRIS crystals were formed.

3.3. Solubility and Dissolution Rate Studies

The solubility of NAP, NAP-EDA and NAP-TRIS salts was determined using ultraviolet spectrophotometry. Given that neither EDA nor TRIS exhibit ultraviolet absorption at 331 nm, the specific absorption of NAP at this wavelength enables its concentration to be measured using ultraviolet spectrophotometry.

The solubility experimental procedure comprises the following steps: Initially, an excess amount of sample was placed in a round-bottom flask containing 10 mL of medium. Subsequently, the flask was positioned on a temperature-controlled magnetic stirrer and agitated for 24 h at 37 ± 0.5 °C. Following this, the mixture was allowed to settle, and the resulting supernatant was filtered through a 0.22 μm filter membrane. Ultimately, the concentration of NAP in the filtrate was determined using ultraviolet spectrophotometry.

The dissolution rate experimental procedure involves the following steps: Initially, 100 mg of the NAP and its salts were accurately weighed and compressed into a tablet with a surface area of 0.5 cm^2 under a pressure of 10 MPa. Subsequently, the dissolution rates of NAP and its salts were assessed under varying medium conditions employing the wet method. During the experiment, a PJ-3 four-in-one tablet testing instrument was utilized, with the rotation speed set at 100 rpm, the temperature maintained at 37 ± 0.5 °C, and a dissolution medium volume of 500 mL. The experiments on solubility and dissolution rate were conducted three times, and the average values were taken.

3.4. Pharmacokinetic Studies

Pharmacokinetic studies were conducted to evaluate the effects of NAP and NAP-TRIS salt in 12 male Sprague-Dawley rats. Each group consisted of six rats, with each rat weighing approximately 250 g. To administer the oral formulations, equimolar quantities of NAP (10.00 mg/kg) and NAP-TRIS (15.26 mg/kg) were given via intragastric administration. Blood samples of approximately 0.5 mL were collected from the eye socket at various time points: 0.5, 1, 2, 4, 6, 8, 12, 24 and 48 h post-administration. These samples were analyzed to determine the concentration of naproxen in plasma.

HPLC was employed to determine the NAP concentration in plasma, using the Agilent 1100 instrument. The HPLC analysis was performed under the following conditions: a flow rate of 1.0 mL/min, a column temperature set at 25 °C, a detection wavelength of 225 nm, an injection volume of 10 μL and a mobile phase consisting of 0.2% phosphoric acid and acetonitrile in a 50:50, v/v ratio, C18 chromatographic column: 250 × 4.6 mm, 5 μm.

4. Conclusions

The hydrophobic groups and naphthalene ring structure of naproxen present significant challenges for enhancing its solubility. This study aims to enhance the water solubility of NAP by employing co-crystal ligands with high solubility in water. We successfully synthesized two new NAP salts, designated as NAP-EDA and NAP-TRIS, through solvent-assisted grinding and slow solvent evaporation techniques. Using single-crystal diffraction techniques, we determined the crystal structures of these two salts and performed a thorough characterization of their physicochemical properties. In comparison to the raw drug naproxen, both NAP-EDA and NAP-TRIS salts demonstrated significantly enhanced solubility and dissolution rates in water and pH 6.86 buffer. Additionally, pharmacokinetic studies in rats indicated that NAP-TRIS salt exhibited a faster absorption rate and higher peak plasma concentration than NAP, which enhanced NAP's oral bioavailability. Therefore, NAP-TRIS salt presents itself as a promising candidate for a new formulation of NAP. This research establishes a crucial basis for predicting the solubility and bioavailability of poorly soluble compounds formed as salts in biologically relevant environments.

Supplementary Materials: The following supporting information can be downloaded at https://www.mdpi.com/article/10.3390/cryst14121104/s1, Figure S1: Observing the chirality diagram of NAP in NAP-EDA from a molecular perspective; Figure S2: The stacking diagram of two independent S-configured NAP molecules in NAP-EDA; Figure S3: Observing the chirality diagram of NAP in NAP-TRIS from a molecular perspective; Figure S4: The stacking diagram of NAP-TRIS; Figure S5: Comparison PXRD patterns of NAP and its residual materials after 24 h solubility in water and pH 6.86 solutions; Figure S6: Comparison PXRD patterns of NAP-EDA and its residual materials after 24 h solubility in water and pH 6.86 solutions; Figure S7: Comparison PXRD patterns of NAP-TRIS and its residual materials after 24 h solubility in water and pH 6.86 solutions.

Author Contributions: Conceptualization, X.-R.Z.; methodology, X.-R.Z.; software, X.-R.Z.; validation, X.-R.Z., B.-L.W. and J.-J.H.; formal analysis, J.-J.H.; investigation, J.-Q.L.; resources, X.-R.Z.; data curation, J.-Q.L.; writing—original draft preparation, X.-R.Z.; writing—review and editing, X.-R.Z.; visualization, B.-L.W.; supervision, B.-L.W.; project administration, X.-R.Z.; funding acquisition, X.-R.Z. All authors have read and agreed to the published version of the manuscript.

Funding: This research was funded by the Guangxi Science and Technology Base and Talent Project (Grant No.: GUIKE AD20159051), Wuzhou University Foundation (Grant No.: 2023B004) and Innovation and Entrepreneurship Training program for College students (202411354048).

Institutional Review Board Statement: Not applicable.

Informed Consent Statement: Not applicable.

Data Availability Statement: The data on the compounds are available from the authors.

Conflicts of Interest: The authors declare no conflicts of interest.

References

1. Karmi-Jafari, M.; Padrela, L.; Walker, G.M.; Croker, D.M. Creating cocrystals: A review of pharmaceutical cocrystal preparation routes and applications. *Cryst. Growth Des.* **2018**, *18*, 6370–6387. [CrossRef]
2. Sun, L.; Wang, Y.; Yang, F.; Zhang, X.; Hu, W. Cocrystal engineering: A collaborative strategy toward functional materials. *Adv. Mater.* **2019**, *31*, 1902328. [CrossRef] [PubMed]
3. Bolla, G.; Sarma, B.; Nangia, A.K. Crystal engineering of pharmaceutical cocrystals in the discovery and development of improved drugs. *Chem. Rev.* **2022**, *122*, 11514–11603. [CrossRef] [PubMed]
4. Bharate, S.S. Recent developments in pharmaceutical salts: FDA approvals from 2015–2019. *Drug Discov. Today* **2021**, *26*, 384–398. [CrossRef]
5. Nugrahani, I.; Parwati, R.D. Challeges and progress in nonsteroidal anti-inflammatory drugs co-crystal development. *Molecules* **2021**, *26*, 4185. [CrossRef]
6. Nangia, A.K.; Desiraju, G.R. Heterosynthons, solid form design and enhanced drug bioavailability. *Angew. Chem. Int. Ed.* **2022**, *134*, e202207484. [CrossRef]
7. Drozd, K.V.; Manin, A.N.; Boycov, D.E.; Perlovich, G.L. Simultaneous improvement of dissolution behavior and oral bioavailability of antifungal miconazole via cocrystal and salt formation. *Pharmaceutics* **2022**, *14*, 1107. [CrossRef]
8. Florindo, C.; Costa, A.; Matos, C.; Nunes, S.L.; Matias, A.N.; Duarte, C.M.M.; Rebelo, L.P.N.; Branco, L.C.; Marrucho, I.M. Novel organic salts based on fluoroquinolone drugs: Synthesis, bioavailability and toxicological profiles. *Int. J. Pharm.* **2014**, *469*, 179–189. [CrossRef]
9. Guo, C.; Wang, Y.; Xie, J.; Zhu, B.; Qi, M.H.; Hong, M.; Ren, G.B. Novel salts of the atypical antipsychotic drug lurasidone with improved solubility and bioavailability. *Cryst. Growth Des.* **2022**, *23*, 326–332. [CrossRef]
10. Gwak, H.S.; Choi, J.S.; Choi, H.K. Enhanced bioavailability of piroxicam via salt formation with ethanolamines. *Int. J. Pharm.* **2005**, *297*, 156–161. [CrossRef]
11. Liu, L.; Zou, Y.; Zhang, Y.; Zhang, D.; Zhang, Y.; Zhang, Q.; Wang, J.; Zeng, S.; Wang, C. Assembly of threepharmaceutical salts/cocrystals of tetrahydroberine with sulfophenyl acids: Improving the properties by formation of charge-assisted hydrogen bonds. *New J. Chem.* **2019**, *43*, 4886–4894. [CrossRef]
12. Berge, S.M.; Bighley, L.D.; Monkhouse, D.C. Pharmaceutical salts. *J. Pharm. Sci.* **1977**, *66*, 1–19. [CrossRef] [PubMed]
13. Serajuddin, A.T. Salt forming to improve drug solubility. *Adv. Drug Deliv. Rev.* **2007**, *59*, 603–616. [CrossRef]
14. Nechipadappu, S.K.; Truvedi, D.R. Pharmaceutical salts of ethionamide with GRAS counter ion donors to enhance the solubility. *Eur. J. Pharm. Sci.* **2017**, *96*, 578–589. [CrossRef]
15. Nechipadappu, S.K.; Reddy, I.R.; Tarafder, K.; Trivedi, D.R. Salt/cocrystal of anti-fibrinolytic hemostatic drug tranexamic acid: Structural, DFT, and stability study of salt/cocrystal with GRAS molecules. *Cryst. Growth Des.* **2018**, *19*, 347–361. [CrossRef]
16. He, S.F.; Zhang, X.R.; Zhang, S.; Guan, S.; Li, J.; Li, S. An investigation into vortioxetine salts: Crystal structure, thermal stability, and solubilization. *J. Pharm. Sci.* **2016**, *105*, 2123–2128. [CrossRef]
17. Li, J.; Li, L.Y.; He, S.F.; Li, S.; Dong, C.Z.; Zhang, L. Crystal structures, X-ray photoelectron spectroscopy, thermodynamic stabilities, and improved solubilities of 2-hydrochloride salts of vortioxetine. *J. Pharm. Sci.* **2017**, *106*, 1069–1074. [CrossRef]
18. Carvalho, P.S.; Diniz, L.F.; Tenorio, J.C.; Souza, M.S.; Franco, C.H.J.; Rial, R.C.; de Oliveira, K.R.W.; Nazario, C.E.D.; Ellena, J. Pharmaceutical paroxetine-based organic salts of carboxylic acids with optimized properties: The identification and characterization of potential novel API solid forms. *CrystEngComm* **2019**, *21*, 3668–3678. [CrossRef]
19. Owoyemi, B.C.D.; da Silva, C.C.; Diniz, L.F.; Souza, M.S.; Ellena, J.; Carneiro, R.L. Fluconazolium oxalate: Synthesis and structural characterization of a highly soluble crystalline form. *CrystEngComm* **2019**, *21*, 1114–1121. [CrossRef]

20. Sanphui, P.; Tothadi, S.; Ganguly, S.; Desiraju, G.R. Salt and cocrystals of sildenafil with dicarboxylic acids: Solubility and pharmacokinetic advantage of the glutarate salt. *Mol. Pharm.* **2013**, *10*, 4687–4697. [CrossRef]
21. Harrington, P.J.; Lodewijk, E. Twenty years of naproxen technology. *Org. Process Res. Dev.* **1997**, *1*, 72–76. [CrossRef]
22. ADAPT Research Group. Naproxen and celecoxib do not prevent AD in early results from a randomized controlled trial. *Neurology* **2007**, *68*, 1800–1808. [CrossRef] [PubMed]
23. Davies, N.M.; Anderson, K.E. Clinical pharmacokinetics of naproxen. *Clin. Pharmacokinet.* **1997**, *32*, 268–293. [CrossRef] [PubMed]
24. Sevelius, H.; Runkel, R.; Segre, E.; Bloomfield, S.S. Bioavailability of naproxen sodium and its relationship to clinical analgestic effects. *Br. J. Clin. Pharmacol.* **1980**, *10*, 259–263. [CrossRef]
25. Calvo, M.V.; Lanao, J.M.; Dominguez-Gil, A. Bioavailability of rectally administered naproxen. *Int. J. Pharm.* **1987**, *38*, 117–122. [CrossRef]
26. Ando, S.; Kikuchi, J.; Fujimura, Y.; Ida, Y.; Higashi, K.; Moribe, K.; Yamamoto, K. Physicochemical characterization and structural evaluation of a specific 2:1 cocrystal of naproxen-nicotinamide. *J. Pharm. Sci.* **2012**, *101*, 3214–3221. [CrossRef]
27. Abbas, N.; Latif, S.; Afzal, H.; Arshad, M.S.; Hussain, A.; Sadeeqa, S.; Bukhari, N.I. Simultaneously improving mechanical, formulation, and in vivo performance of naproxen by co-crystallization. *AAPS PharmSciTech* **2018**, *19*, 3249–3257. [CrossRef]
28. Kim, H.; Jang, S.; Kim, I.W. Enhanced dissolution of naproxen by combining cocrystallization and eutectic formation. *Pharmaceutics* **2021**, *13*, 618. [CrossRef]
29. Kerr, H.E.; Softley, L.K.; Suresh, K.; Hodgkinson, P.; Evans, I.R. Structure and physicochemical characterization of a naproxen-picolinamide cocrystal. *Acta Crystallogr. C* **2017**, *73*, 168–175. [CrossRef]
30. Skorupska, E.; Jeziorna, A.; Potrzebowski, M.J. Thermal solvent-free method of loading of pharmaceutical cocrystals into the pores of silica particles: A case of naproxen/picolinamide cocrystal. *J. Phys. Chem. C* **2016**, *120*, 13169–13180. [CrossRef]
31. Buschmann, H.H.; Sola, C.; Buchholz, J.B.; Bertran, J.C. Co-Crystals of Duloxetine and Co-Crystal Formers for the Treatment of Pain. European Patent EP2123626A1, 25 November 2009.
32. Latif, S.; Ijaz, Q.A.; Hameed, M.; Shoaib, Q.U.; Fatima, K.; Hussain, A.; Arshad, M.S.; Abbas, N. Improvement of physico-mechanical and pharmacokinetic attributes of naproxen by cocrystallization with L-alanine. *J. Drug Deliv. Sci. Technol.* **2021**, *61*, 102236. [CrossRef]
33. Tumanova, N.; Tumanov, N.; Robeyns, K.; Filinchuk, Y.; Wouters, J.; Leyssens, T. Structural insight into cocrystallization with zwitterionic co-formers: Cocrystals of S-naproxen. *CrystEngComm* **2014**, *16*, 8185–8196. [CrossRef]
34. Kasten, G.; Lobo, L.; Dengale, S.; Grohganz, H.; Rades, T.; Löbmann, K. In vitro and in vivo comparison between crystalline and co-amorphous salts of naproxen-arginine. *Eur. J. Pharm. Biopharm.* **2018**, *132*, 192–199. [CrossRef] [PubMed]
35. Tilborg, A.; Springuel, G.; Norberg, B.; Wouters, J.; Leyssens, T. On the influence of using a zwitterionic coformer for cocrystallization: Structural focus on naproxen-proline cocrystals. *CrystEngComm* **2013**, *15*, 3341–3350. [CrossRef]
36. Heinrich, B.H.; Lluis, S.C.; Jordi, B.B.; Carles, C.B.J.; Ramon, P.; Nicolas, T. Co-Crystals of Tramadol and NSAIDs. Japan Pantent JP5645830B2, 24 December 2014.
37. Manoj, K.; Tamura, R.; Takahashi, H.; Tsue, H. Crystal engineering of homochiral molecular organization of naproxen in cocrystals and their thermal phase transformation studies. *CrystEngComm* **2014**, *16*, 5811–5819. [CrossRef]
38. Nechipadappu, S.K.; Trivedi, D.R. Structural and physicochemical characterization of pyridine derivative salts of anti-inflammatory drugs. *J. Mol. Struct.* **2017**, *1141*, 64–74. [CrossRef]
39. Rajurkar, V.G.; Gite, R.D.; Ghawate, V.B. Development of naproxen cocrystal formation: An efficient approach to enhance aqueous solubility. *Anal. Chem. Lett.* **2015**, *5*, 229–238. [CrossRef]
40. Fu, Q.; Lu, H.D.; Xie, Y.F.; Liu, J.Y.; Han, Y.; Gong, N.B.; Guo, F. Salt formation of two BCS II drugs (indomethacin and naproxen) with (1R,2R)-1,2-diphenylethylenediamine: Crystal structures, solubility and thermodynamics analysis. *J. Mol. Struct.* **2019**, *1185*, 281–289. [CrossRef]
41. Xing, C.; Chen, T.; Wang, L.; An, Q.; Jin, Y.; Yang, D.; Zhang, L.; Du, G.; Lu, Y. Two novel co-crystals of naproxen: Comparison of stability, solubility and intermolecular interaction. *Pharmaceuticals* **2022**, *15*, 807. [CrossRef]
42. Zhang, X.; Gao, Y. A novel drug-drug salt of naproxen and vortioxetine: Synthesis, characterization, and solubility study. *J. Chem.* **2023**, *2023*, 6678252. [CrossRef]
43. Yuliandra, Y.; Izadihari, R.; Rosaini, H.; Zaini, E. Multicomponent crystals of mefenamic acid-tromethamine with improved dissolution rate. *J. Res. Pharm.* **2019**, *23*, 988–996. [CrossRef]
44. Bruni, G.; Berbenni, V.; Maggi, L.; Mustarelli, P.; Friuli, V.; Ferrara, C.; Pardi, F.; Castagna, F.; Girella, A.; Milanese, C. Multicomponent crystals of gliclazide and tromethamine: Preparation, physico-chemical, and pharmaceutical characterization. *Drug Dev. Ind. Pharm.* **2018**, *44*, 243–250. [CrossRef] [PubMed]
45. Bookwala, M.; Thipsay, P.; Ross, S.; Zhang, F.; Bandari, S.; Repka, M.A. Preparation of a crystalline salt of indomethacin and tromethamine by hot melt extrusion technology. *Eur. J. Pharm. Biopharm.* **2018**, *131*, 109–119. [CrossRef] [PubMed]
46. Greenwood, D.; Coyle, S.; Andrew, J. The trometamol salt of fosfomycin: Microbiological evaluation. *Eur. Urol.* **1987**, *13*, 69–75. [CrossRef]
47. Fitriani, L.; Firdaus, W.A.; Sidadang, W.; Rosaini, H.; Putra, O.D.; Oyama, H.; Uekusa, H.; Zaini, E. Improved solubility and dissolution rate of ketoprofen by the formation of multicomponent crystals with tromethamine. *Crystals* **2022**, *12*, 275. [CrossRef]

48. Rossi, P.; Paoli, P.; Milazzo, S.; Chelazzi, L.; Giovannoni, M.P.; Guerrini, G.; Lenco, A.; Valleri, M.; Conti, L. A combined crystallographic and computational study on dexketoprofen trometamol dehydrate salt. *Crystals* **2020**, *10*, 659. [CrossRef]
49. Sheldrick, G.M. SHELXT-Integrated space-group and crystal-structure determination. *Acta Cryst. A* **2015**, *71*, 3–8. [CrossRef]
50. Pennington, W.T. Diamond-visual crystal structure information system. *J. Appl. Crystallogr.* **1999**, *32*, 1028–1029. [CrossRef]

Disclaimer/Publisher's Note: The statements, opinions and data contained in all publications are solely those of the individual author(s) and contributor(s) and not of MDPI and/or the editor(s). MDPI and/or the editor(s) disclaim responsibility for any injury to people or property resulting from any ideas, methods, instructions or products referred to in the content.